Bioorg. Med. Chem. 46 (2021) 116355

Contents lists available at ScienceDirect

Bioorganic & Medicinal Chemistry

journal homepage: www.elsevier.com/locate/bmc

Evaluation of γ-carboline-phenothiazine conjugates as simultaneous NMDA receptor blockers and cholinesterase inhibitors

Sigrid Schwarthoff [a], Nicolas Tischer [a], Henrike Sager [a], Bianca Schätz [a], Marius M. Rohrbach [a], Ihar Raztsou [b], Dina Robaa [c], Friedemann Gaube [a], Hans-Dieter Arndt [b], Thomas Winckler [a,*]

[a] Institute of Pharmacy, Pharmaceutical Biology, University of Jena, Semmelweisstrasse 10, 07743 Jena, Germany
[b] Institute of Organic Chemistry and Macromolecular Chemistry, University of Jena, Humboldtstrasse 10, 07743 Jena, Germany
[c] Institute of Pharmacy, Martin Luther University Halle-Wittenberg, Wolfgang-Langenbeck-Strasse 4, 06120 Halle/Saale, Germany

ARTICLE INFO

Keywords:
Alzheimer's disease
Multitarget ligand
Carboline
AChE
BChE
NMDA receptor

ABSTRACT

Alzheimer's disease (AD) is the most common form of dementia. It is associated with the impairment of memory and other cognitive functions that are mainly caused by progressive defects in cholinergic and glutamatergic signaling in the central nervous system. Inhibitors of acetylcholinesterase (AChE) and ionotropic glutamate receptors of the *N*-methyl-D-aspartate (NMDA) receptor family are currently approved as AD therapeutics. We previously showed using a cell-based assay of NMDA receptor-mediated glutamate-induced excitotoxicity that *bis*-γ-carbolinium conjugates are useful NMDA receptor blockers. However, these compounds also act as subnanomolar AChE inhibitors, which may cause serious anticholinergic side effects when applied *in vivo*. Here, we evaluated new structures containing γ-carbolines linked to phenothiazine via a propionyl spacer. These compounds were superior to the previously characterized *bis*-γ-carbolinium conjugates because they blocked NMDA receptors without requiring a quaternary pyridine *N*-atom and inhibited AChE with moderate IC_{50} values of 0.54–5.3 μM. In addition, these new compounds displayed considerable selectivity for the inhibition of butyrylcholinesterase (BChE; IC_{50} = 0.008–0.041 μM), which may be favorable for AD treatment. Inhibitory activities towards the NMDA receptors and AChE were in the same micromolar range, which may be beneficial for equal dosing against multiple targets in AD patients.

1. Introduction

Neurodegenerative disorders pose a major challenge to 21st century health systems. It was estimated in the World Alzheimer Report 2019 that more than 50 million people are currently living with dementia, and more than 150 million people may be affected by 2050.[1] Alzheimer's disease (AD) is the most common form of dementia and is associated with the progressive impairment of memory and other cognitive functions.[2–4] The cerebrovascular pathology of AD is complex, and causal therapy is missing. Progressive defects in cholinergic and glutamatergic signaling in the central nervous system are mainly responsible for the loss of cognitive functions; therefore, disease-modifying or symptomatic treatments that slow disease progression for a certain period of time are usable. Among the currently approved drugs for the treatment of AD are AChE inhibitors such as donepezil, rivastigmine and galantamine and the NMDA receptor blocker memantine.

Acetylcholine can be hydrolyzed by either AChE or BChE. Although BChE appears to play a minor role in regulating brain acetylcholine levels in the healthy brain, its level progressively increases in late AD pathology, while the activity of AChE drastically declines at the same time. BChE has been found in amyloid plaques and neurofibrillary tangles, suggesting that the enzyme may not only be important for regulating acetylcholinergic neurotransmission but also directly contribute to AD pathogenesis. Thus, an increasing body of evidence points to a critical role of BChE in AD pathogenesis and suggests that there is therapeutic value in drugs that inhibit BChE more strongly than AChE.[5–9]

Because AChE inhibitors and memantine address different clinical targets, it is tempting to evaluate the potential of drug combinations for the therapy of AD.[10] Although controversially discussed, several clinical trials have suggested that the combination of an AChE inhibitor with memantine may be superior to AChE inhibitor monotherapy.[11–15] We

Abbreviations: AChE, acetylcholinesterase; AD, Alzheimer's disease; BChE, butyrylcholinesterase; NMDA, *N*-methyl-D-aspartat.

* Corresponding author.
E-mail address: t.winckler@uni-jena.de (T. Winckler).

https://doi.org/10.1016/j.bmc.2021.116355
Received 15 May 2021; Received in revised form 19 July 2021; Accepted 30 July 2021
Available online 8 August 2021

previously showed that *bis*-γ-carbolinium conjugate **1** (Fig. 1) acts as an NMDA receptor blocker in an NMDA receptor-mediated, glutamate-induced excitotoxicity assay in cells expressing recombinant GluN1-1a/2A or GluN1-1a/2B receptors and in patch clamp assays on recombinant cells expressing GluN1-1a/2A receptors.[16] Interestingly, **1** is also a very strong AChE inhibitor with a subnanomolar IC_{50} for the inhibition of both AChE and BChE,[16] which may be unfavorable for therapy because it may provoke serious central anticholinergic side effects. Thus, multifunctional compounds based on γ-carboline fragments have potential as single-molecule combination therapeutics for the treatment of AD, yet compounds with moderate AChE-inhibiting properties and relative selectivity for BChE inhibition may provide a better therapeutic option.

We have consistently observed that simple (monomeric) γ-carbolines are unable to block NMDA receptors in a cell assay of glutamate-induced excitotoxicity. On the other hand, homobivalent γ-carboline conjugates critically require *N*-alkylation of the pyridine *N*-atom (**1**) to act as NMDA receptor blockers, whereas unmethylated derivatives (**2**) or tetrahydro-γ-carboline conjugates (**3**) are completely inactive.[16,18] Interestingly, Makhaeva *et al.* recently reported that tetrahydro-γ-carbolines conjugated with phenothiazine, as realized in compound **4** (Fig. 1), displayed affinity in ligand binding assays for NMDA receptors prepared from the membranes of mouse hippocampi.[17] We found this result surprising because compound **4** does not contain a quaternary ammonium ion in the γ-carboline moiety and presumably would not be functional as an NMDA receptor blocker in our glutamate-induced excitotoxicity assay. Therefore, we were interested in independently synthesizing **4** and determining whether it blocked NMDA receptors in our assay. In addition, we wanted to explore whether derivatives of compound **4** could be developed into NMDA receptor blockers if the alkylated piperidine in **4** was replaced by an alkylated pyridine, as in **1**. Another interesting aspect of the report by Makhaeva *et al.* was that compound **4** appeared to act as a selective BChE inhibitor ($IC_{50} = 1.07$ μM) and was reported to be inactive against human AChE with an $IC_{50} > 200$ μM.[17] Therefore, we also determined the inhibitory potency of the new γ-carboline-phenothiazine conjugates against AChE and BChE.

2. Results and discussion

2.1. Carboline-phenothiazine conjugates are NMDA receptor blockers.

Makhaeva *et al.* reported that conjugate **4** reduced the binding of the specific ligands [^{3}H]MK-801 and [^{3}H]ifenprodil from hippocampal NMDA receptors with IC_{50} values of 18.5 μM and 23.4 μM, respectively, and suggested that **4** is an NMDA receptor blocker.[17] In our assay of NMDA receptor-mediated, glutamate-induced excitotoxicity, monomeric tetrahydro-γ-carbolines or compounds composed of two tetrahydro-γ-carbolines, such as **3**, have never displayed meaningful NMDA receptor-blocking activity.[16,18] Compound **4** differs from our previously evaluated homobivalent carbolines in that it is not linked to another carboline but instead conjugated with a phenothiazine fragment, and this linkage is facilitated via a short propionyl spacer instead of a long flexible nonamethylene linker, as in **1**–**3**. Therefore, we were interested in determining whether a tetrahydro-γ-carboline in the context of heterobivalent phenothiazine conjugates produced NMDA receptor blocking properties in our functional assay.

To generate γ-carboline-phenothiazine conjugates, we first synthesized γ-carboline scaffolds by using Fischer indole synthesis of 1-benzyl-piperidin-4-en with phenylhydrazine, which led to the tetrahydro-γ-carbolines **5** (Scheme 1). Aromatization of tetrahydro-γ-carbolines of series **5** and debenzylation provided the γ-carbolines of series **6**. Conjugation of the γ-carbolines **6** with phenothiazine by a propionyl spacer yielded the compounds of series **7**. Alkylation of the γ-carbolines **7** led to pyridinium salts **8**. Compound **8a** was partially reduced with $NaBH_4$ to obtain **4** (Scheme 1).

Unfortunately, in contrast to the report by Makhaeva [18], compound **4** did not reduce NMDA receptor-mediated excitotoxicity to more than 50% in our assay at concentrations up to 50 μM. This seemed to confirm our previous observations that γ-carboline conjugates bearing partially reduced carboline fragments are generally poor NMDA receptor blockers. However, we wondered whether it would be possible to convert **4** into a functional NMDA blocker by transforming it into a fully aromatized carboline (series **7**). These derivatives were further modified by alkylation of the pyridine *N*-atom to yield compounds bearing a permanent positive charge (series **8**). We also added different substituents at position 8 of the γ-carboline scaffold. Such modifications might prevent metabolism of this vulnerable aromatic position *in vivo*. We then compared the activities of γ-carboline-phenothiazine conjugates **7** and **8** with the respective monomeric carbolines **5**, **6**, **9** and **10** in the cell-based glutamate-induced excitotoxicity assay (Table 1). None of the monomeric compounds, including phenothiazine, showed significant NMDA receptor blocking activity. In contrast, all compounds in series **7** and **8** inhibited glutamate-induced excitotoxicity with IC_{50} values in the low micromolar range, comparable with the standard of care, the drug memantine. The most active compounds **7d** and **8d** had activities comparable to the previously evaluated homobivalent γ-carbolinium **1**. Surprisingly, the series **7** compounds inhibited glutamate-induced excitotoxicity with potencies similar to the series **8** compounds, even though they lacked a quaternary pyridine *N*-atom. Concerning the modifications of series **7** and **8** compounds at position 8, there was a trend towards stronger NMDA receptor blocking activities with methyl (**7c**, **8c**) and methoxy residues (**7d**, **8d**) compared with either a proton (**7a, 8a**) or F-atom (**7b**, **8b**). Bulkier alkyl groups on the pyridine *N*-atom of the γ-carboline (methyl **8a** versus benzyl **8e**) did not notably affect the NMDA receptor-blocking activity of the γ-carboline-phenothiazine conjugates. In summary, our assays revealed that **7d** and **8d** were quite promising NMDA receptor blockers that differed markedly in their permanent positive charge on the pyridine *N*-atom. The observation that **7d** blocked NMDA receptors with an efficacy similar to that of **1** and of **8d** is promising for future *in vivo* applications because the neutral pyridine **7d** may be able to cross the blood–brain barrier more efficiently than the positively charged compounds.

The γ-carboline-phenothiazine conjugates of series **7** and **8** were found to be effective NMDA receptor blockers, even though the

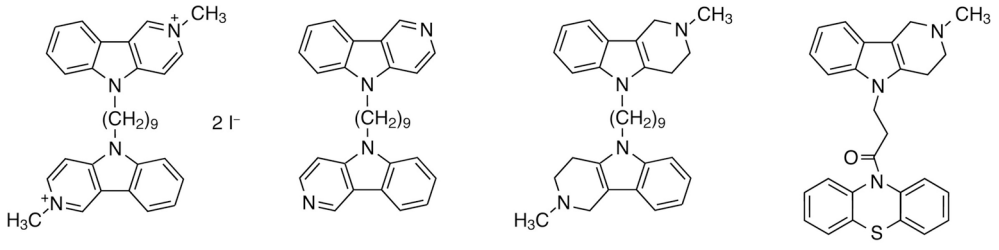

1 **2** **3** **4**

Fig. 1. Previously known compounds. The homobivalent γ-carboline conjugates **1**–**3** (16) and the γ-carboline-phenothiazine conjugate **4** (17) were used for comparison with the new compounds described in this study.

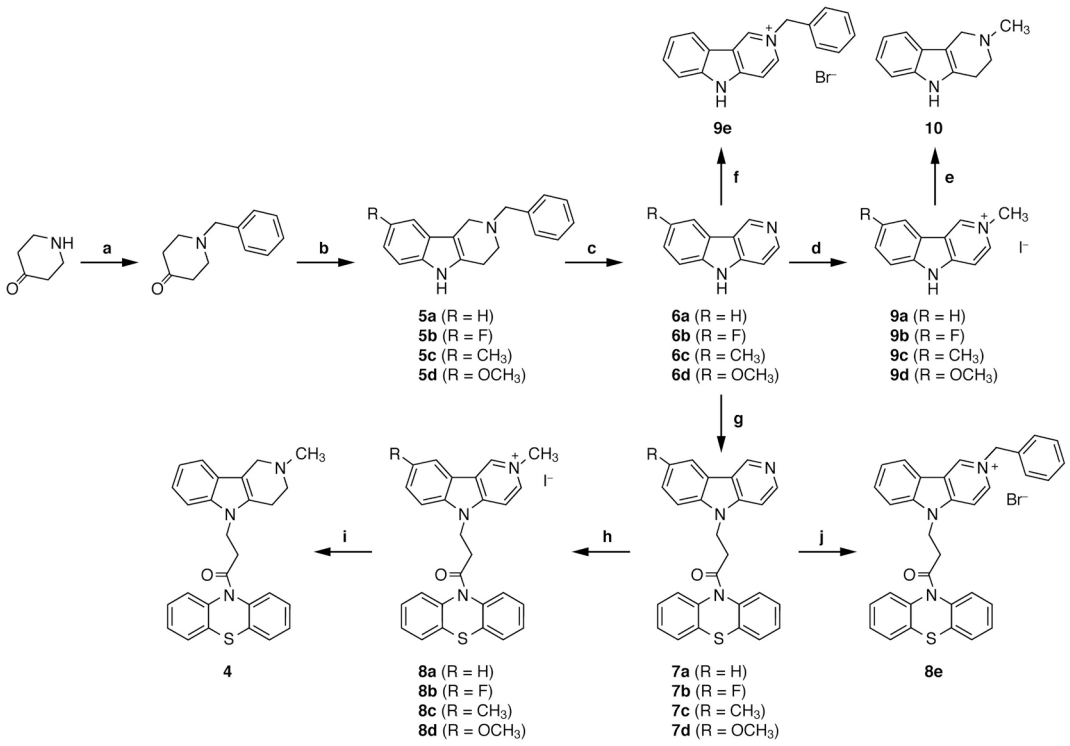

Scheme 1. Synthesis of compounds evaluated in this study. a) Benzyl bromide, K_2CO_3, CH_2Cl_2, 12 h, r.t., 74%. b) 4-R-Phenylhydrazine, H_2SO_4, dioxane, 2 h, 60 °C, 73% for R = H, 75% for R = F, 45% for R = Me, 52% for R = MeO. c) Pd/C (10%), toluene, 12 h, reflux, 25% for R = H, 10% for R = F, 94% for R = Me, 90% for R = MeO. d) MeI, THF, 12 h, r.t., R = H: detailed in[18], 67% for R = F, 88% for R = Me, 48% for R = MeO. e) Detailed in[18]. f) For R = H: benzyl bromide, acetone, 12 h, r.t., 13%. g) For R = H: 3-bromo-1-(10*H*-phenothiazin-10-yl)propan-1-one, NaOH, DMSO, 4 h, r.t., 42%. For R = F: 3-bromo-1-(10*H*-phenothiazin-10-yl)propan-1-one, KO^{t}Bu, THF, 24 h, r.t., 9%. For R = Me/MeO: 3-bromo-1-(10*H*-phenothiazin-10-yl)propan-1-one, KO^{t}Bu, CH_3CN, 12 h, r.t., 36% for R = Me, 33% for R = MeO. h) MeI, THF, 89% for R = H, 69% for R = F, 79% for R = Me, 77% for R = MeO. i) For R = H: $NaBH_4$, MeOH, 4 h, 43%. j) For R = H: benzyl bromide, acetone, 12 h, r. t., 44%.

monomeric γ-carbolines and phenothiazine alone displayed negligible efficacy. This finding implied that linking γ-carbolines with phenothiazine into a composite molecule generated compounds with new pharmacological properties. To further substantiate this observation, we performed an assay of glutamate-induced excitotoxicity and added different γ-carboline monomers alone or in combination with phenothiazine (10 μM each) to NMDA receptor-expressing cells. We compared these data with the effects of the γ-carboline-phenothiazine conjugates of series **7** and **8**. As expected, monomeric γ-carbolines alone had no considerable NMDA receptor-blocking activity (Fig. 2). Phenothiazine had a moderate effect (27% inhibition) on glutamate-induced excitotoxicity in this particular experiment. Mixing a monomeric γ-carboline with phenothiazine (10 μM each) did not enhance the moderate inhibition of glutamate-induced excitotoxicity caused by phenothiazine. In contrast, the γ-carboline-phenothiazine conjugates at 10 μM were significantly superior to the γ-carboline-phenothiazine mixture (Fig. 2). Thus, the γ-carboline and phenothiazine scaffolds create novel pharmacological entities when connected to a single molecule.

2.2. Carboline-phenothiazine conjugates act as cholinesterase inhibitors.

We previously used commercial AChE from *Electrophorus electricus* to predict the potential of homobivalent γ-carbolines to inhibit human AChE.[16] Because several amino acids of the active-site gorges are conserved between human AChE and enzymes from nonhuman sources, such as *Torpedo* or *Electrophorus*, inhibition of nonhuman AChE is a good predictor for the initial screening of inhibitors of human AChE.[19] Nevertheless, detailed deviations in the sequence along the active site gorge might favor the human enzyme for drug development.[20] However, commercial sources of recombinant human AChE or preparations of human erythrocytes are extremely costly, whereas routine preparation of hAChE from whole blood is laborious. Therefore, we decided to produce recombinant human AChE in-house as an enzyme source to further characterize the γ-carboline conjugates. To this end, we cloned the coding sequence of human erythrocyte AChE including the authentic amino-terminal signal peptide sequence (GenBank accession number M55040) into the pcDNA3.1 expression vector and selected stable cell lines after transfection of HEK293 cells. Medium from serum-free cultivation of transgenic HEK293 cells was collected and used as source of recombinant human AChE (rhAChE). Compound **1** inhibited rhAChE with an IC_{50} of 0.33 nM (Table 1), which is comparable to the previously determined inhibition of *Electrophorus* AChE (IC_{50} = 0.45 nM;[16]), suggesting that rhAChE is a reliable replacement for *Electrophorus* AChE.

Makhaeva *et al.* previously reported that **4** did not inhibit commercially available AChE prepared from human erythrocytes (IC_{50} > 200 μM), but did inhibit equine BChE with an IC_{50} of 1.07 μM.[17] Based on these data, the authors concluded that **4** is a selective BChE inhibitor. In our hands, however, **4** inhibited rhAChE with an IC_{50} of 7.8 μM and equine BChE with an IC_{50} of 0.17 μM (Table 1). To address the divergent hAChE inhibition data, we confirmed our results with an independent source of human AChE. To this end, we prepared blood erythrocytes from volunteer blood donors and used membrane-bound human AChE as an enzyme source. The erythrocyte AChE preparation was first tested with our model structure **1**, which inhibited the enzyme with an IC_{50} of 0.40 nM. This was close to the data obtained for the soluble rhAChE (IC_{50} = 0.33 nM) (Fig. 3A). Compound **7a** also had comparable inhibitory activity against rhAChE (IC_{50} = 2.3 ± 0.3 μM) and erythrocyte AChE (IC_{50} = 3.5 ± 0.6 μM), as did **8a** (IC_{50} = 2.2 ± 0.8 μM and 5.5 ± 2.3 μM, respectively). These data suggested that both rhAChE and human erythrocyte AChE are equally reliable sources for the characterization of AChE inhibitors. Notably, **4** was active against human

Table 1
Inhibition of NMDA receptor-mediated glutamate-induced excitotoxicity and cholinesterases by γ-carbolines and γ-carboline conjugates.

Compound	NMDAR GluN1-1a/2A IC_{50} [μM] ± SD	NMDAR GluN1-1a/2B IC_{50} [μM] ± SD	rhAChE IC_{50} [μM] ± SD	BChE IC_{50} [μM] ± SD
1	0.4 ± 0.05[a]	0.8 ± 0.09[a]	0.00033 ± 0.00025	0.016 ± 0.001[a]
2	n.a.[a,b]	n.a.[a,b]	0.08 ± 0.02	0.013 ± 0.001[a]
3	n.a.[a,b]	n.a.[a,b]	n.d.	0.052 ± 0.008[a]
4	n.a.[b]	n.a.[b]	7.8 ± 0.5	0.170 ± 0.02
5a	n.a.[b]	n.a.[b]	20.4 ± 4.9	6.5 ± 0.09
5b	n.a.[c]	n.a.[c]	17.6 ± 6.2	2.1 ± 0.05
5c	n.a.[b]	n.a.[b]	35.1 ± 1.6	1.4 ± 0.3
5d	n.a.[b]	n.a.[b]	52.7 ± 5.9	6.3 ± 1.4
6a	n.a.[b]	n.a.[b]	21.4 ± 2.6	1.2 ± 0.05
6b	n.a.[b]	n.a.[b]	11.4 ± 2.4	0.55 ± 0.03
6c	n.a.[b]	n.a.[b]	35.4 ± 4.3	1.4 ± 0.6
6d	n.a.[b]	n.a.[b]	49.6 ± 6.1	12.6 ± 2.3
7a	4.2 ± 1.4	3.0 ± 0.8	2.3 ± 0.3	0.008 ± 0.001
7b	1.7 ± 0.3	2.7 ± 0.3	6.2 ± 1.0	0.008 ± 0.001
7c	1.3 ± 0.3	1.5 ± 0.4	0.51 ± 0.25	0.016 ± 0.005
7d	0.8 ± 0.1	0.6 ± 0.04	0.54 ± 0.09	0.037 ± 0.005
8a	2.4 ± 1.0	1.4 ± 0.9	2.2 ± 0.8	0.041 ± 0.003
8b	3.0 ± 0.2	2.1 ± 1.0	2.6 ± 0.2	0.032 ± 0.002
8c	0.9 ± 0.4	0.5 ± 0.2	1.1 ± 0.4	0.032 ± 0.001
8d	0.4 ± 0.1	0.2 ± 0.05	5.3 ± 1.6	0.041 ± 0.003
8e	1.0 ± 0.3	0.9 ± 0.1	2.2 ± 1.1	0.011 ± 0.002
9a	n.a.[b]	n.a.[b]	8.7 ± 2.4	0.89 ± 0.24
9b	n.a.[b]	n.a.[b]	1.9 ± 0.9	2.7 ± 0.4
9c	n.a.[a,b]	n.a.[b]	9.1 ± 2.6	5.5 ± 0.3
9d	n.a.[b]	n.a.[b]	14.7 ± 2.8	9.8 ± 0.2
9e	n.a.[b]	n.a.[b]	8.6 ± 1.8	1.9 ± 0.1
10	n.a.[b]	n.a.[b]	n.a.[b]	6.5 ± 0.1
Donepezil	n.d.	n.d.	0.0049 ± 0.001	1.3 ± 0.2
Phenothiazine	n.a.[d]	n.a.[d]	n.a.[d]	n.a.[d]
Memantine	6.7 ± 3.3	6.0 ± 1.7	n.d.	n.d.

[a] Data from[16].
[b] n.a., not active (<50% inhibition at 50 μM; IC_{50} not determined due to insufficient solubility at ≥ 50 μM).
[c] n.a., not active (<50% inhibition at 20 μM; IC_{50} not determined due to insufficient solubility at > 20 μM in buffer).
[d] n.a., < 30% inhibition at 20 μM; IC_{50} could not be determined due to insufficient solubility at > 20 μM in buffer; n.d., not determined.

erythrocyte AChE (IC_{50} of 24.4 μM) and displayed full inhibition at concentrations > 100 μM (Fig. 3B). Thus, in our hands, tetrahydro-γ-carboline-phenothiazine conjugates such as **4** are moderate AChE inhibitors and cannot be considered BChE-selective inhibitors.

Monomeric γ-carbolines (series **5**, **6**, **9** and **10**) inhibited both AChE and BChE in the micromolar range, yet they were generally far less potent than the conjugates consisting of either two carbolines or a carboline and a phenothiazine (Table 1). The γ-carboline-phenothiazine conjugates of series **7** had AChE inhibitory activities similar to those of the aromatic homobivalent γ-carboline **2** (e.g., IC_{50} = 2.3 μM for **7a** and 0.08 μM for **2**) but were considerably more potent than monomer **6a** (IC_{50} = 21.4 ± 2.6; Table 1). This suggested that the phenothiazine moiety of the molecule contributed significantly to the binding to AChE. The weakening of the AChE inhibitory activity of the quaternary γ-carboline-phenothiazine conjugates (series **8**) compared with homobivalent γ-carboline **1** was very pronounced, with **1** being 6600-fold more active against AChE than **8a** (Table 1). Nevertheless, the γ-carboline-phenothiazine conjugates displayed a certain preference for BChE over AChE, whereas the homobivalent γ-carbolines were moderately AChE-selective. This result was mainly attributed to the loss in AChE inhibitory activity rather than BChE inhibition, which remained in the nanomolar range (Table 1). In summary, **7b** was identified as an interesting candidate for further evaluation because it displayed 775-fold selectivity for BChE (IC_{50} = 0.008 μM for BChE and IC_{50} = 6.2 μM for AChE).

We performed docking studies to identify structural factors for the moderate selectivity of the γ-carboline-phenothiazine conjugates for BChE over AChE. Because we used equine BChE as an enzyme source in our experiments, we first generated a homology model of equine BChE (UniProt Q9N1N9) based on the crystal structure of human BChE in complex with tacrine (PDB 4BDS). All γ-carboline-phenothiazine conjugates showed a similar binding mode. The γ-carboline moiety was positioned into the choline binding site of BChE, where it was stabilized by π-π stacking interactions with Trp110. The protonated amine of tetrahydro-γ-carboline **4** showed an additional salt bridge interaction with Glu225 and cation-π interactions with Trp110 (Fig. 4A). Similarly, an ionic interaction with Glu225 and a cation-π interaction with Trp110 were observed for the *N*-methylated derivatives **8** (Fig. 4B, C). Moreover, the phenothiazine scaffold of derivatives **4, 7** and **8** was embedded in the acyl binding pocket and adopted the same binding conformation as it was previously observed for the phenothiazine moiety of ethopropazine (PDB 6EQP).[21] The phenothiazine group showed π-π stacking interactions with Trp259 and Tyr360 as well as van der Waals interactions with Leu313 and Leu314. Unfortunately, docking did not reveal an obvious explanation for the increased inhibitory activity of derivatives **7** and **8** compared to tetrahydrocarboline derivative **4**. Entropic contributions and solvation/desolvation effects might play a role, which cannot be accounted for properly by molecular docking.

Docking of the homobivalent derivatives, as exemplified by **1** (Fig. 4D), showed one γ-carboline group embedded in the choline binding site of BChE, where it was stabilized by π-π stacking interactions with Trp110 and ionic interactions with Glu225. In contrast to the γ-carboline-phenothiazine conjugates **4, 7** and **8**, the second tricyclic moiety of the bivalent derivatives does not reside in the acyl binding site but rather extends into the peripheral site, showing only van der Waals interactions with Leu313 and Leu314.

It has been observed that the active site gorges of AChE and BChE are considerably different; six out of the 14 aromatic acid residues lining the AChE gorge are replaced by aliphatic amino acid residues in BChE.[21,22] Compared to AChE, the acyl binding pocket of BChE has been shown to allow for the binding of bulkier ligands, mainly due to four amino acid mutations: Tyr120, Phe288, Phe290, and Phe330 of AChE from *Torpedo californica* (TcAChE), which are replaced by Gln147, Leu314, Val316, and Ala314 in equine BChE. Indeed, polycyclic aromatic compounds such as ethopropazine were found to show significant selectivity for BChE over AChE, since they can be accommodated in the acyl binding pocket of BChE but are not able to bind to AChE in a similar manner.[21]

Comparison of the available crystal structures revealed that the peripheral anionic site (PAS) of AChE can undergo significant conformational changes upon binding to different ligands. The Trp279-Ser291 loop (TcAChE numbering), which encompasses the acyl binding pocket as well as PAS residues, was found to adapt to different conformations that consequently impacted the accessibility of the PAS. Binding of the bivalent ligand NF595, for instance, was accompanied by a significant conformational change in the PAS, especially the side chain conformation of Trp297.[23–25] Additionally, significant structural plasticity of Phe330 and Phe331 was observed, which similarly affects the shape and accessibility of the PAS.[26] Human AChE and TcAChE show 80% sequence identity and 95% sequence similarity in the binding gorge. The crystal structure of TcAChE in complex with a bis-tacrine inhibitor (PDB 2CKM) provided a good model for predicting the binding of the bivalent

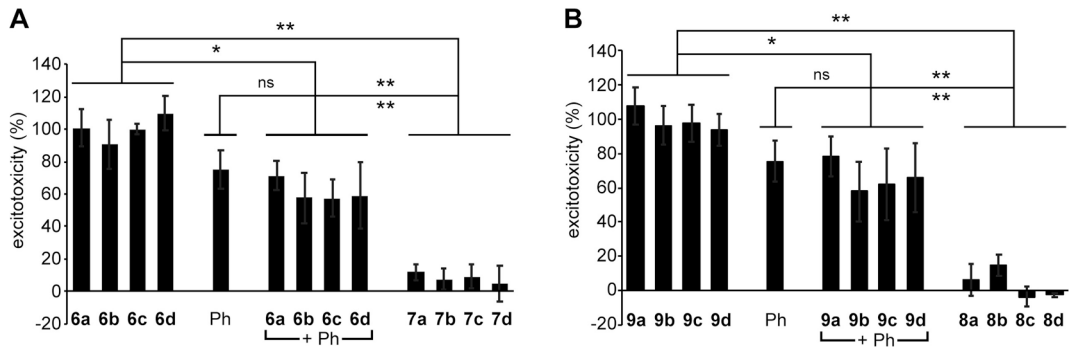

Fig. 2. Synergistic action of the pharmacophores of the γ-carboline conjugates. Monomeric carbolines of series **6** (panel A) and **9** (panel B) were tested in cells expressing GluN1-1a/2A receptors for their ability to inhibit glutamate-induced excitotoxicity. Carbolines and phenothiazine (Ph) were tested alone or as γ-carboline-phenothiazine combinations, and inhibitory activities were compared with the respective γ-carboline-phenothiazine conjugates of series **7** or **8**. All test compounds were added at a final concentration of 10 μM. Values are the means of at least three experiments ± SD (Student's *t*-test; ns: not significant ($p > 0.05$); *: $p < 0.05$; **: $p < 0.01$). Similar results were obtained using cells expressing GluN1-1a/2B receptors (data not shown).

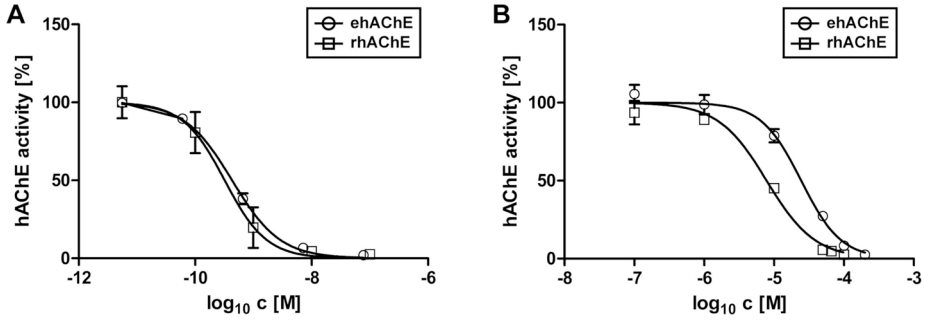

Fig. 3. Inhibitory effects of γ-carbolines on human AChE. Inhibition of recombinantly produced human AChE (rhAChE) and AChE prepared from human erythrocytes (ehAChE) by **1** (panel A) and **4** (panel B).

carboline-based inhibitors evaluated in this study. Therefore, even though we experimentally examined γ-carbolines as inhibitors of human AChE, we preferred to predict their binding to AChE based on the model of TcAChE in docking studies.

As expected, the docking results revealed that the conjugate γ-carboline-phenothiazine derivatives did not fit well in the AChE active gorge. While the γ-carboline moiety in **4, 7** and **8** can still be placed in the choline binding site, the bulky phenothiazine moiety cannot be accommodated in the acyl binding site and instead projects out of the active site gorge into a solvent-exposed hydrophilic pocket (Fig. 5A). Moreover, the bivalent γ-carboline derivatives **1**–**3** show the same binding mode as it was observed for the analogous bivalent tacrine derivatives.[26] One γ-carboline group is sandwiched between Trp279 and Tyr70 in the choline binding site, where it participates in π-π stacking interactions (Fig. 5B). Additionally, the protonated amine of tetrahydro-γ-carboline derivative **3** and the quaternary ammonium group of **1** display cation-π interactions with the surrounding aromatic acid residues and an ionic interaction with Glu278. The second γ-carboline moiety binds in the PAS, showing π-π stacking interactions with Trp84 and Tyr330 as well as cation-π and ionic interactions in the case of derivatives **1** and **3**.

In summary, these docking results revealed key factors for the relative selectivity for BChE inhibition over AChE inhibition and provided a rationale for the decrease from subnanomolar to micromolar affinities for AChE of the homobivalent γ-carbolines to the heterobivalent γ-carboline-phenothiazine conjugates.

3. Conclusions

Alzheimer's disease is a multifactorial form of dementia that may be most effectively treated with combination therapy that addresses several targets in parallel. In this study, we showed that conjugation of γ-carboline and phenothiazine fragments results in molecules with new pharmacological properties that can inhibit AChE and block NMDA receptors at similar micromolar concentrations, suggesting that these compounds may be beneficial for equal dosing against multiple targets in AD patients. The most interesting γ-carboline-phenothiazine conjugate **7b** had 775-fold selectivity for cholinesterase inhibition (IC_{50} = 0.008 μM for BChE and IC_{50} = 6.2 μM for AChE), suggesting that this compound is an interesting candidate for further evaluation of a single molecule multitargeted ligand for AD therapy.

4. Experimental section

4.1. Chemistry

All reagents were commercially available and used without further purification. All solvents used were distilled or analytical grade. ^{1}H- and ^{13}C NMR spectra were recorded using a Bruker Avance I 250 system (250 MHz for ^{1}H NMR), a Bruker Fourier 300 system (300 MHz for ^{1}H NMR) or a Bruker Avance IV (NEO) system (126 MHz for ^{13}C NMR). High-resolution mass spectra (ESI-TOF) were obtained on a maXis Impact mass spectrometer (Bruker Daltronik, Bremen, Germany). Purity of compounds was determined by HPLC using a Macherey Nagel 760101.40 EC 250/4 Nucleodur C18 Gravity, 5 μm column. ^{1}H NMR, ^{13}C NMR and HPLC methods and spectra are provided in the Supplementary Material.

4.1.1. Homobivalent γ-carbolines (1–3)

The synthesis of homobivalent γ-carbolines **1**–**3** has been described elsewhere [16].

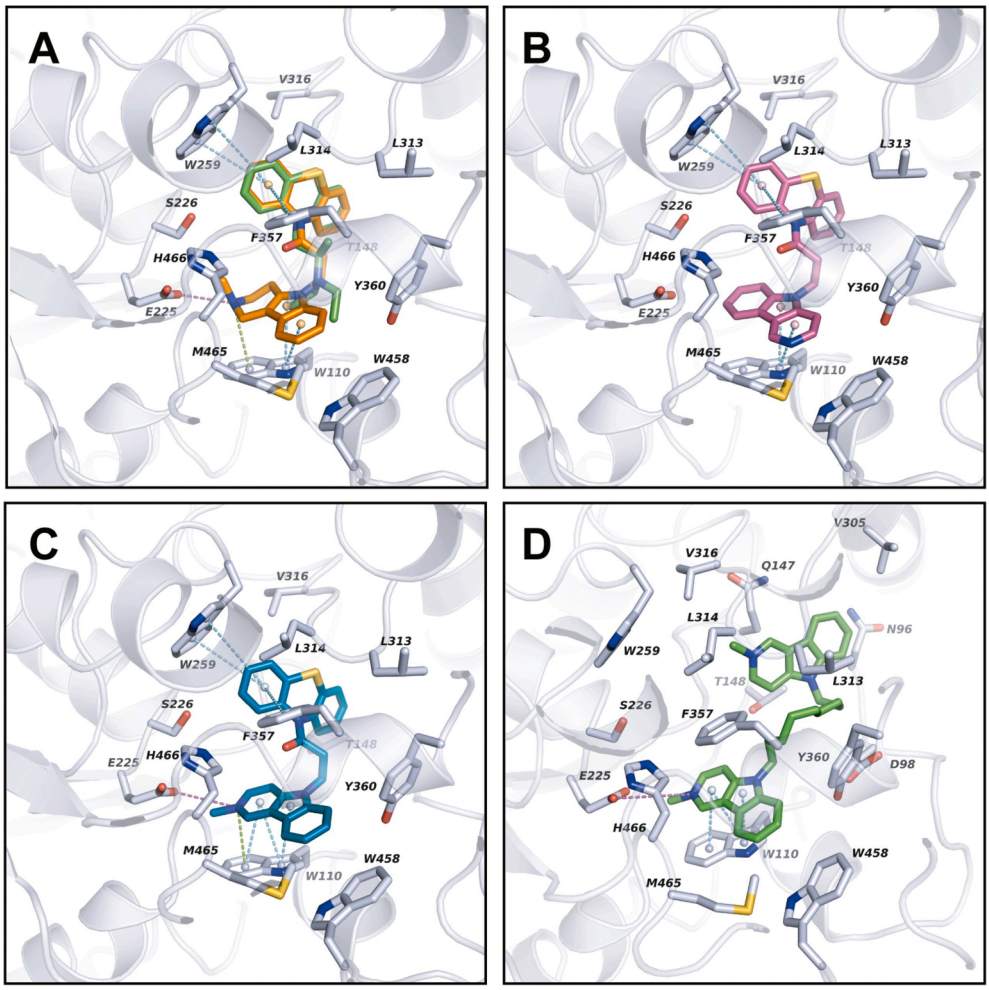

Fig. 4. Binding of γ-carboline derivatives to BChE. A) Predicted binding mode of **4** (orange sticks) in equine BChE overlaid with the experimentally determined binding mode of ethopropazine (green sticks). B) Predicted binding mode of **7a** (purple sticks). C) Predicted binding mode of **8a** (teal sticks). D) Obtained docking pose of **1** (green sticks) in equine BChE. Residues lining the active site gorge are shown as white sticks, π-π-stacking interactions are shown as cyan dashed lines, cation-π interactions as green dashed lines and ionic interactions as purple dashed lines. Water molecules are omitted. (For interpretation of the references to color in this figure legend, the reader is referred to the web version of this article.)

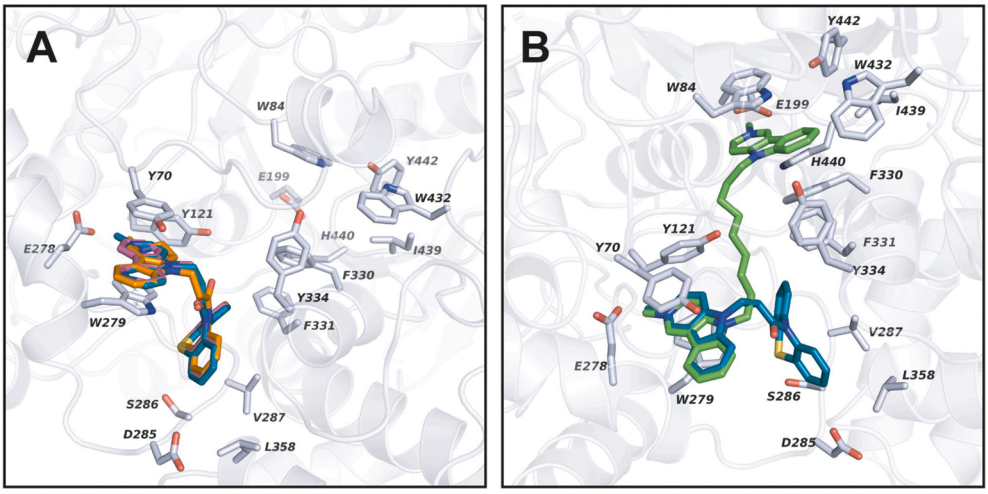

Fig. 5. Binding of γ-carboline derivatives to AChE. A) Obtained docking poses of **4** (orange sticks), **7a** (teal sticks), and **8a** (purple sticks) in TcAChE (PDB 2CKM). Residues lining the active site gorge are shown as white sticks, and π-π-stacking interactions are shown as cyan dashed lines. Water molecules are omitted. B) Overlay of the docking poses obtained for **1** (green sticks) and **7a** (teal sticks) in the binding pocket of AChE. (For interpretation of the references to color in this figure legend, the reader is referred to the web version of this article.)

*4.1.2. Synthesis of compound **4***

Compound **4** was first described in.[17] In this study, we used the synthesis route described below.

3-(2-Methyl-1,2,3,4-tetrahydro-5H-pyrido[4,3-b]indole-5-yl)-1-(10H-phenothiazine-10-yl)propane-1-one (**4**). To a cooled solution of compound **8a** (100 mg, 0.18 mmol, 1 equiv.) in methanol (20 mL) sodium borohydride (7 mg, 0.18 mmol, 1 equiv.) was added. The resulting solution was stirred at room temperature for 3 h. Water (40 mL) was added, and the methanol was removed under reduced pressure. The aqueous phase was extracted with dichloromethane (3 × 40 mL). The combined organic extracts were dried with sodium sulfate and concentrated under reduced pressure. The resulting light brown foam was purified by chromatography on silica gel (SiO_2 40–63 µm, CH_2Cl_2-MeOH 6:1) to furnish 33.5 mg (76.2 µmol, 43%) of pale-yellow oil (**4**), R_f 0.75 (CH_2Cl_2-MeOH, 6:1).

t_R 9.31 min (Method B). ^{1}H NMR ($CDCl_3$, 300 MHz) δ = 7.1–7.5 (m, 12H, H-6, H-7, H-8, H-9, phenothiazine-H), 4.37 (br s, 2H, N—$\underline{CH_2}$—CH_2), 4.09 (s, 2H, H-1), 3.1–3.2 (m, 2H, $\underline{CH_2}$—C═O), 3.07 (br s, 2H, H-3), 2.91 (br s, 2H, H-4), 2.71 (s, 3H, methyl-H). ^{13}C NMR (75 MHz, $CDCl_3$) δ = 169.64, 138.01, 136.12, 131.16, 127.95, 127.23, 127.10, 125.43, 121.87, 119.81, 117.77, 109.17, 103.90, 77.25, 51.63, 51.24, 43.23, 39.58, 34.03, 20.31. HPLC/HRMS $[M+H]^+$ for $C_{26}H_{23}N_3OS$ calculated 440.1791, found 440.1795.

4.1.3. Synthesis of compounds series 5

General procedure. Benzyl bromide (316 mg, 1.85 mmol, 1 equiv.) was added to a solution of 4-piperidone monohydrate hydrochloride (283 mg, 1.85 mmol) in 30 mL dichloromethane and 2 mL methanol and stirred for 12 h. Then, the organic phase was washed with water (3 × 30 mL) and dried with sodium sulfate. The crude product was purified by chromatography on silica gel (SiO_2 40–63 µm, PE – EtOAc 3:1) to furnish 1-benzylpiperidine-4-one as a pale-yellow oil (260 mg, 1.37 mmol, 74%), R_f 0.15. ^{1}H NMR (300 MHz, $CDCl_3$) δ = 7.27–7.41 (m, 5H), 3.64 (s, 2H), 2.76 (t, J = 6.15 Hz, 4H), 2.43–2.51 (m, 4H) ppm.

The synthesis of the tetrahydro-γ-carboline scaffold was performed as described[27]: 1-benzylpiperidine-4-one was dissolved in 1,4-dioxane, and one equivalent of 4-phenylhydrazine for **5a** or the corresponding substituted derivative was added. To this solution, 3.5 equivalents of concentrated sulfuric acid were added, and the reaction solution was heated to 60 °C for three hours. After full conversion was monitored by TLC, the solution was cooled down to room temperature, and saturated $NaHCO_3$-solution and solid NaOH were added to the solution to adjust pH 13. The aqueous phase was extracted with ethyl acetate (4 × 0.5 vol of the aqueous phase), and the combined organic layers were washed with brine and dried with sodium sulfate. The crude product was purified by chromatography on silica gel yielding **5a** or the substituted derivatives **5b-d**, respectively.

2-Benzyl-2,3,4,5-tetrahydro-1H-pyrido[4,3-b]indole (**5a**). Yield 73%. R_f = 0.55 (CH_2Cl_2-MeOH, 20:1). t_R 6.55 min (Method B). ^{1}H NMR (300 MHz, $CDCl_3$), δ = 7.82 (br s, 1H, H-5), 7.03–7.48 (m, 9H, H-6, H-7, H-8, H-9, benzyl-H), 3.83 (s, 2H, H-1), 3.76 (s, 2H, benzyl-H), 2.81–2.95 (m, 4H, H-3, H-4). ^{13}C NMR (75 MHz, $CDCl_3$) δ = 138.74, 136.02, 132.13, 129.12, 128.33, 127.12, 126.19, 121.15, 119.27, 117.59, 110.54, 108.90, 77.23, 62.37, 50.10, 49.82, 23.80. HPLC/HRMS $[M+H]^+$ for $C_{18}H_{18}N_2$ calculated 263.1543, found 263.1549.

2-Benzyl-8-fluoro-2,3,4,5-tetrahydro-1H-pyrido[4,3-b]indole (**5b**). Yield 75%. R_f = 0.33 (CH_2Cl_2-MeOH, 15:1). t_R 6.92 min (Method B). ^{1}H NMR (300 MHz, $CDCl_3$) δ = 8.00 (br s, 1H, H-5), 7.46–6.84 (m, 8H, H-6, H-7, H-9, benzyl-H), 3.58–3.74 (m, 2H, H-1) 3.82 (s, 2H, benzyl-H), 2.99–2.74 (m, 4H, H-3, H-4). ^{13}C NMR (126 MHz, $CDCl_3$) δ = 158.65, 156.80, 138.26, 134.09, 132.45, 129.16, 128.38, 127.25, 126.48, 126.40, 110.99, 110.91, 109.19, 108.98, 102.84, 102.66, 62.31, 49.96, 49.60, 23.81. HPLC/HRMS $[M+H]^+$ for $C_{18}H_{17}FN_2$ calculated 281.1449, found 281.1452.

2-Benzyl-8-methyl-2,3,4,5-tetrahydro-1H-pyrido[4,3-b]indole (**5c**). Yield 45%. R_f = 0.58 (CH_2Cl_2-MeOH, 9:1). t_R 7.45 min (Method B). ^{1}H NMR (300 MHz, $CDCl_3$), δ = 8.7 (s, 1H, H-5), 6.85–7.6 (m, 8H, H-6, H-7, H-9, benzyl-H), 3.8–4.05 (m, 4H, H-1, benzyl-H), 3.05–3.2 (m, 2H, H-3), 2.9–3.0 (m, 2H, H-4), 2.4 (s, 3H, methyl-H). ^{13}C NMR (126 MHz, $CDCl_3$) δ = 138.51, 134.31, 132.12, 129.16, 128.42, 128.31, 127.14, 126.38, 122.58, 117.39, 110.16, 108.21, 62.27, 50.13, 49.74, 23.70, 21.43. HPLC/HRMS $[M+H]^+$ for $C_{19}H_{20}N_2$ calculated 276.1669, found 277.1701.

2-Benzyl-8-methoxy-2,3,4,5-tetrahydro-1H-pyrido[4,3-b]indole (**5d**). Yield 52%. R_f = 0.36 (CH_2Cl_2-MeOH, 9:1). t_R 6.24 min (Method B). ^{1}H NMR (250 MHz, $CDCl_3$), δ = 7.92 (br s, 1H, H-5), 7.17–7.52 (m, 6H, H-6, benzyl-H), 6.76–6.81 (m, 2H, H-7, H-9), 3.71–3.95 (m, 7H, H-1, benzyl-H, methoxy-H), 2.74–3.10 (m, 4H, H-3, H-4). ^{13}C NMR (126 MHz, $CDCl_3$) δ = 153.89, 138.53, 132.95, 131.07, 129.13, 128.33, 127.15, 126.50, 111.17, 110.78, 108.55, 99.97, 62.31, 55.88, 50.13, 49.77, 23.78.

4.1.4. Synthesis of compounds series 6

General procedure. For aromatization and debenzylation of tetrahydro-γ-carboline, **5a** or the substituted derivative **5b-d** was dissolved in toluene, Pd/C (10 m%) was added, and the suspension was heated to reflux for 24 h. A 0.3-fold volume of warm methanol was added to the warm suspension, which was then filtrated. The filtrate was concentrated under reduced pressure, purified by chromatography on silica gel, and dried, yielding 2-benzyl-2,3,4,5-tetrahydro-1*H*-pyrido[4,3-*b*]indole or the corresponding substituted derivative.

5H-Pyrido[4,3-b]indole (**6a**). Yield 25%. R_f = 0.56 (CH_2Cl_2-MeOH, 9:1). t_R 7.17 min (Method A). ^{1}H NMR (CD_3OD, 300 MHz) δ = 9.19 (s, 1H, H-1), 8.35 (d, 1H, J = 5.9 Hz, H-3), 8.15 (d, 1H, J = 7.8 Hz, H-9), 7.4–7.6 (m, 3H, H-4, H-6, H-7), 7.28 (t, 1H, J = 7.5 Hz, H-8). ^{13}C NMR (126 MHz, CD_3OD) δ = 145.95, 144.57, 142.86, 141.63, 128.30, 122.55, 121.78, 121.71, 121.67, 112.56, 107.73. HPLC/HRMS $[M+H]^+$ for $C_{11}H_8N_2$ calculated 169.0760, found 169.0761.

8-Fluoro-5H-pyrido[4,3-b]indole (**6b**). Yield 10%. R_f = 0.47 (CH_2Cl_2-MeOH, 20:1). t_R 7.60 min (Method A). ^{1}H NMR (CD_3OD, 250 MHz) δ = 9.23 (s, 1H, H-1), 8.39 (d, 1H, J = 5.9 Hz, H-3), 7.93 (dd, 1H, J = 2.6, 9.0 Hz, H-9), 7.4–7.6 (m, 2H, H-4, H-6), 7.29 (dt, 1H, J = 2.4, 9.1 Hz, H-7). ^{13}C NMR (126 MHz, CD_3OD) δ = 160.54, 158.67, 146.86, 144.93, 143.46, 137.98, 123.27, 123.19, 121.50, 121.47, 116.15, 115.95, 113.54, 113.47, 107.96, 107.43, 107.24. HPLC/HRMS $[M+H]^+$ for $C_{11}H_7FN_2$ calculated 187.0666, found 187.0669.

8-Methyl-5H-pyrido[4,3-b]indole (**6c**). Yield 94%. R_f = 0.22 (CH_2Cl_2-MeOH, 12:1). t_R 8.20 min (Method A). ^{1}H NMR (DMSO-d_6, 300 MHz) δ = 11.57 (br s, 1H, H-5), 9.27 (s, 1H, H-1), 8.37 (br d, 1H, J = 5.6 Hz, H-3), 8.00 (s, 1H, H-9), 7.3–7.5 (m, 2H, H-6, H-7), 7.28 (br d, 1H, J = 8.3 Hz, H-4), 2.4–2.5 (m, 3H, methyl-H). ^{13}C NMR (126 MHz, CD_3OD) δ = 146.12, 144.33, 142.74, 139.82, 131.34, 129.65, 122.73, 121.57, 121.46, 112.25, 107.66, 21.60. HPLC/HRMS $[M+H]^+$ for $C_{12}H_{10}N_2$ calculated 183.0817, found 183.0917.

8-Methoxy-5H-pyrido[4,3-b]indole (**6d**). Yield 90%. R_f = 0.25 (CH_2Cl_2-MeOH 9:1). t_R 7.60 min (Method A). ^{1}H NMR (CD_3OD, 400 MHz) δ = 9.19 (s, 1H, H-1), 8.32 (d, 1H, J = 5.8 Hz, H-3), 7.72 (d, 1H, J = 2.6 Hz, H-9), 7.4–7.5 (m, 2H, H-4, H-6), 7.13 (dd, 1H, J = 2.6, 8.8 Hz, H-7), 3.9–4.0 (m, 3H, methoxy-H). ^{13}C NMR (126 MHz, CD_3OD) δ = 156.38, 146.32, 144.27, 143.03, 136.30, 123.09, 121.76, 117.73, 113.27, 107.73, 104.24, 56.51. HPLC/HRMS $[M+H]^+$ for $C_{12}H_{10}N_2O$ calculated 199.0866, found 199.0870.

4.1.5. Synthesis of compounds series 7

General procedure. 3-Bromo-1-(10H-phenothiazine-10-yl)propane-1-one: The strategy of Sardessi *et al.*[28] was applied as follows: To a solution of 10*H*-phenothiazine (1.00 g, 5.00 mmol) in toluene (80 mL), 3-bromopropanoyl chloride (858 mg, 5.00 mmol) was added dropwise under a nitrogen atmosphere. The reaction mixture was heated to reflux for 24 h, cooled to room temperature, and poured into ice water (100 mL). Layers were separated; the organic layer was washed with 10% $NaHCO_3$ solution (100 mL), water (100 mL), and saturated NaCl solution (100 mL). Removal of the solvent under reduced pressure gave a green solid residue, which was recrystallized from toluene-hexane to afford 3-bromo-1-(10*H*-phenothiazine-10-yl)propane-1-one (1.6 g, 4.6 mmol, 91%) as a dark green crystalline solid.

Different conditions had to be applied to connect this fragment with the γ-carboline derivatives **6a-d**. In general, the γ-carboline was deprotonated, and one equivalent of 3-bromo-1-(10*H*-phenothiazine-10-yl)propane-1-one was added. The reaction was stopped after full conversion of the starting material (monitoring by TLC), and the product purified by chromatography on silica gel.

1-(10H-Phenothiazine-10-yl)-3-(5H-pyrido[4,3-b]indole-5-yl)propane-1-one **(7a)**. For linking the γ-carboline **6a** to 3-bromo-1-(10*H*-phenothiazine-10-yl)propane-1-one, the solvent and base were chosen as described in (16). A solution of 5*H*-pyrido[4,3-*b*]indole **6a** (100 mg, 600 µmol, 1 equiv.) and NaOH (24 mg, 600 µmol, 1 equiv.) in DMSO (10 mL) was stirred for 1 h. After addition of 3-bromo-1-(10*H*-phenothiazine-10-

yl)propane-1-one (200 mg, 600 μmol, 1 equiv.), the reaction mixture was stirred for another 4 h and then poured into water (16 mL). The solution was extracted with chloroform (2 × 10 mL). The organic phase was concentrated under reduced pressure. The resulting green oil was lyophilized and purified by chromatography on silica gel (SiO_2 40–63 μm, CH_2Cl_2-MeOH 11:1) to furnish **7a** (105 mg, 249.3 μmol, 42%) as pale-yellow crystalline solid, R_f 0.50 (CH_2Cl_2-MeOH, 11:1). t_R 8.53 min (Method B). ^{1}H NMR ($CDCl_3$, 300 MHz) δ = 9.3–9.3 (m, 1H, H-1), 8.54 (d, 1H, J = 5.9 Hz, H-3), 8.17 (d, 1H, J = 7.7 Hz, H-6), 7.4–7.6 (m, 1H, H-4), 7.1–7.4 (m, 11*H*, H-7, H-8, H-9, phenothiazine-H), 4.68 (br s, 2H, N—CH_2—CH_2), 3.00 (br s, 2H, CH_2—C═O). ^{13}C NMR (126 MHz, $CDCl_3$) δ = 169.54, 144.66, 144.27, 142.38, 139.87, 137.99, 128.00, 127.09, 127.04, 121.53, 120.93, 120.84, 119.79, 109.23, 104.34, 39.59, 32.94. HPLC/HRMS $[M+H]^+$ for $C_{26}H_{19}N_3OS$ calculated 422.1322, found 422.1325.

3-(8-Fluoro-5H-pyrido[4,3-b]indole-5-yl)-1-(10H-phenothiazine-10-yl) propane-1-one (**7b**). A solution of **6b** (300 mg, 1.60 mmol, 1 equiv.) and potassium 2-methylpropane-2-olate (180 mg, 1.6 mmol, 1 equiv.) in THF (40 mL) was stirred for 1 h. After addition of 3-bromo-1-(10*H*-phenothiazine-10-yl)propane-1-one (535 mg, 1.6 mmol, 1 equiv.), the reaction mixture was stirred for 48 h. The solvent was removed under reduced pressure, and the crude product was purified by chromatography on silica gel (SiO_2 40–63 μm, CH_2Cl_2-MeOH 20/12:1) to furnish **7b** (64 mg, 0.146 mmol, 9%) as pale-yellow crystalline solid, R_f 0.62 (CH_2Cl_2-MeOH, 10:1). t_R 8.55 min (Method B). ^{1}H NMR ($CDCl_3$, 400 MHz) δ = 9.34 (s, 1H, H-1), 8.47 (br d, 1H, J = 6.4 Hz, H-3), 7.2–7.8 (m, 12H, H-4, H-6, H-7, H-9, phenothiazine-H), 4.7–4.9 (m, 2H, N—CH_2—CH_2), 3.1–3.3 (m, 2H, CH_2—C═O). ^{13}C NMR (126 MHz, $CDCl_3$) δ = 169.47, 159.21, 157.32, 145.04, 144.75, 142.49, 138.27, 137.93, 136.27, 128.03, 127.65, 127.59, 127.09, 126.97, 126.86, 126.64, 115.02, 114.82, 110.11, 110.03, 106.87, 106.82, 106.67, 104.60, 39.83, 32.85. HPLC/HRMS $[M+H]^+$ for $C_{26}H_{18}FN_3OS$ calculated 440.1227, found 440.1229.

3-(8-Methyl-5H-pyrido[4,3-b]indole-5-yl)-1-(10H-phenothiazine-10-yl)propane-1-one (**7c**). A solution of **6c** (419 mg, 2.30 mmol, 1 equiv.) and potassium 2-methylpropane-2-olate (256 mg, 2.30 mmol, 1 equiv.) in acetonitrile (250 mL) was stirred for 1 h. After addition of 3-bromo-1-(10*H*-phenothiazine-10-yl)propane-1-one (770 mg, 2.3 mmol, 1 equiv.), the reaction mixture was stirred for 24 h. Then, the reaction solution was poured into water (250 mL) and extracted with chloroform (2 × 150 mL). The organic layer was concentrated under reduced pressure, and the crude product purified by chromatography on silica gel (SiO_2 40–63 μm, CH_2Cl_2-MeOH 20:1, 40:1) to furnish **7c** (366.4 mg, 0.84 mmol, 36%) as light-brown crystalline solid, R_f 0.25 (CH_2Cl_2-MeOH, 20:1). t_R 9.20 min (Method B). ^{1}H NMR ($CDCl_3$, 250 MHz) δ = 9.28 (s, 1H, H-1), 8.49 (br d, 1H, J = 5.7 Hz, H-3), 7.98 (s, 1H, H-6), 7.1–7.5 (m, 10*H*, H-7, H-9, phenothiazine-H), 4.66 (br s, 2H, N—CH_2—CH_2), 2.9–3.2 (m, 2H, CH_2—C═O), 2.58 (s, 3H, methyl-H). ^{13}C NMR (126 MHz, $CDCl_3$) δ = 169.55, 144.50, 144.35, 142.32, 138.12, 138.02, 130.45, 128.30, 128.00, 127.08, 121.67, 120.77, 119.62, 108.91, 104.25, 39.56, 32.99, 21.33. HPLC/HRMS $[M+H]^+$ for $C_{27}H_{21}N_3OS$ calculated 436.1478, found 436.1477.

3-(8-Methoxy-5H-pyrido[4,3-b]indole-5-yl)-1-(10H-phenothiazine-10-yl)propane-1-one (**7d**). A solution of **6d** (50 mg, 0.252 mmol, 1 equiv.) and potassium 2-methylpropane-2-olate (28 mg, 0.252 mmol, 1 equiv.) in acetonitrile (20 mL) was stirred for 1 h. After addition of 3-bromo-1-(10*H*-phenothiazine-10-yl)propane-1-one (85 mg, 0.252 mmol, 1 equiv.), the reaction mixture was stirred for 24 h. Then, the reaction solution was poured into water (10 mL) and extracted with chloroform (2 × 6 mL). The organic layer was concentrated under reduced pressure, and the crude product was purified by chromatography on silica gel (SiO_2 40–63 μm, CH_2Cl_2-MeOH 20:1) to furnish **7d** (38 mg, 0.084 mmol, 33%) as a slightly pink oil, R_f 0.55 (CH_2Cl_2-MeOH, 20:1). t_R 8.63 min (Method B). ^{1}H NMR ($CDCl_3$, 300 MHz) δ = 9.28 (s, 1H, H-1), 8.50 (d, 1H, J = 5.8 Hz, H-3), 7.0–7.7 (m, 12H, H-4, H-6, H-7, H-9, phenothiazine-H), 4.65 (br s, 2H, N—CH_2—CH_2), 3.96 (s, 3H, methoxy-H), 2.97 (br s, 2H, CH_2—C═O). ^{13}C NMR (126 MHz, $CDCl_3$) δ = 169.56, 155.00, 144.55, 144.22, 142.22, 137.99, 134.70, 128.00, 127.08, 122.03, 119.70, 116.27, 110.09, 104.41, 103.52, 56.06, 39.72, 32.99. HPLC/HRMS $[M+H]^+$ for $C_{27}H_{21}N_3O_2S$ calculated 452.1427, found 452.1435.

4.1.6. Synthesis of compounds series 8

General procedure. All derivatives except compound **8e** were prepared according to the following procedure: To a solution of the corresponding derivate **7** in THF, 10 equivalents of iodomethane were added. The reaction solution was stirred for 12 h. The solvent was removed under reduced pressure and the residue was washed with ice-cold diethyl ether. The yellow crystalline solid was dried under reduced pressure.

2-Methyl-5-(3-oxo-3-(10H-phenothiazine-10-yl)propyl)-5H-pyrido [4,3-b]indole-2-ium iodide (**8a**).Yield 89%. t_R 8.71 min (Method B). ^{1}H NMR (DMSO-d_6, 300 MHz) δ = 9.77 (s, 1H, H-1), 8.67 (dd, 1H, J = 1.2, 7.1 Hz, H-3), 8.35 (d, 1H, J = 7.7 Hz, H-9), 8.16 (d, 1H, J = 7.1 Hz, H-6), 7.68–7.8 (m, 2H, H-7, H-8), 7.2–7.6 (m, 9H, H-4, phenothiazine-H), 4.82 (br t, 2H, J = 6.1 Hz, N—CH_2—CH_2), 4.34 (s, 3H, methyl-H), 3.12 (br s, 2H, CH_2—C═O). ^{13}C NMR (126 MHz, CD_3CN) δ = 170.49, 146.87, 142.88, 139.63, 139.11, 130.79, 128.82, 128.32, 128.17, 124.40, 122.95, 121.63, 121.47, 112.57, 108.72, 47.87, 41.68, 33.20. HPLC/HRMS $[M]^+$ for $C_{27}H_{22}N_3OS^+$ calculated 436.1478, found 436.1483.

8-Fluoro-2-methyl-5-(3-oxo-3-(10H-phenothiazine-10-yl)propyl)-5H-pyrido[4,3-b]indole-2-ium iodide (**8b**). Yield 69%. t_R 8.75 min (Method B). ^{1}H NMR (DMSO-d_6, 400 MHz) δ = 9.76 (s, 1H, H-1), 8.69 (br s, 1H, H-3), 8.1–8.4 (m, 2H, H-6, H-9), 7.3–7.86 (m, 10*H*, H-4, H-7, phenothiazine-H), 4.83 (br s, 2H, N—CH_2—CH_2), 4.35 (br s, 3H, methyl-H), 3.15 (br s, 2H, CH_2—C═O). ^{13}C NMR (126 MHz, CD_3CN) δ = 170.50, 161.12, 159.22, 147.47, 139.90, 139.33, 139.12, 128.80, 128.36, 128.17, 122.44, 122.35, 121.17, 121.13, 118.75, 118.54, 114.17, 114.10, 109.07, 109.03, 108.82, 47.95, 41.97, 33.14. HPLC/HRMS: $[M]^+$ for $C_{27}H_{21}FN_3OS^+$ calculated 454.1384, found 454.1386.

2,8-Dimethyl-5-(3-oxo-3-(10H-phenothiazine-10-yl)propyl)-5H-pyrido [4,3-b]indole-2-ium iodide (**8c**). Yield 79%. t_R 9.47 min (Method B). ^{1}H NMR (DMSO-d_6, 250 MHz) δ = 9.72 (s, 1H, H-1), 8.65 (d, 1H, J = 6.4 Hz, H-3), 8.1–8.2 (m, 2H, H-6, H-9), 7.69 (d, 1H, J = 8.4 Hz, H-4), 7.2–7.6 (m, 9H, H-7, phenothiazine-H), 4.81 (br t, 2H, J = 6.2 Hz, N—CH_2—CH_2), 4.34 (s, 3H, N-CH_3), 3.08 (br d, 2H, J = 18.3 Hz, CH_2—C═O), 2.5–2.6 (m, 3H, C-CH_3). ^{13}C NMR (126 MHz, CD_3CN) δ = 170.51, 146.79, 141.12, 139.37, 138.83, 134.52, 132.16, 128.85, 128.17, 122.52, 121.64, 121.47, 112.29, 108.58, 47.82, 41.68, 33.20, 21.45. HPLC/HRMS $[M]^+$ for $C_{28}H_{24}N_3OS^+$ calculated 450.1635, found 450.1634.

8-Methoxy-2-methyl-5-(3-oxo-3-(10H-phenothiazine-10-yl)propyl)-5H-pyrido[4,3-b]indole-2-ium iodide (**8d**). Yield 77%. t_R 8.77 min (Method B). ^{1}H NMR (CD_3CN, 300 MHz) δ = 9.3–9.4 (m, 1H, H-1), 8.2–8.3 (m, 1H, H-3), 7.7–7.9 (m, 2H, H-6, H-9), 7.2–7.6 (m, 10*H*, H-4, H-7, phenothiazine-H), 4.6–4.8 (m, 2H, N—CH_2—CH_2), 3.9–4.0 (m, 3H, O—CH_3), 3.9–4.0 (m, 3H, N—CH_3), 3.16 (br s, 2H, CH_2—C═O). ^{13}C NMR (CD_3CN, 126 MHz) δ = 170.52, 157.60, 146.62, 139.25, 139.17, 139.10, 137.36, 128.83, 128.33, 128.17, 122.39, 121.44, 119.83, 113.48, 108.64, 105.47, 56.87, 47.81, 41.77, 33.27. HPLC/HRMS $[M]^+$ for $C_{28}H_{24}N_3O_2S^+$ calculated 466.1589, found 466.1589.

2-Benzyl-5-(3-oxo-3-(10H-phenothiazine-10-yl)propyl)-5H-pyrido[4,3-b]indole-2-ium bromide (**8e**). To a solution of 63 mg compound **7a** (149 μmol, 1 equiv.) in acetone, 5 equivalents of benzyl bromide (127 mg, 754 μmol) were added. The reaction solution was stirred for 12 h, the resulting white precipitate was filtered, washed with ice cold acetone yielding **8e** (39 mg, 65.8 μmol, 44%) as colorless crystalline solid, t_R 10.69 min (Method B). ^{1}H NMR (DMSO-d_6, 400 MHz) δ = 10.24 (s, 1H, H-1), 8.89 (m, 1H, H-3), 8.22 (m, 1H, H-9), 8.17 (m, 1H, H-6), 7.19–7.77 (m, 16H, H-7, H-8, H-9, phenothiazine-H, benzyl-H), 5.84 (br s, 2H, benzyl-H), 4.82 (br s, 2H, N—CH_2—CH_2), 3.15 (br s, 2H, CH_2—C═O). ^{13}C NMR (126 MHz, CD_3CN) δ = 170.61, 148.62, 147.19, 142.99,

138.72, 138.38, 130.92, 130.53, 130.48, 129.71, 128.18, 128.14, 124.55, 123.14, 112.58, 109.09, 64.10, 41.93, 32.99. HPLC/HRMS $[M]^+$ for $C_{33}H_{26}N_3OS^+$ calculated 512.1791, found 512.1798.

4.1.7. Synthesis of compounds series 9

General procedure. For the methylation of γ-carboline derivatives, methyl iodide was added to a solution of the derivative in THF. The mixture was stirred for 12 h, then the solvent was removed under reduced pressure, and the residue was washed with ice-cold diethyl ether. The yellow crystalline solid was dried under reduced pressure.

2-Methyl-5H-pyrido[4,3-b]indole-2-ium iodide (**9a**). Detailed in[18].

8-Fluoro-2-methyl-5H-pyrido[4,3-b]indole-2-ium iodide (**9b**). Yield 67%. t_R 7.63 min (Method A). ^{1}H NMR (DMSO-d_6, 300 MHz) δ = 13.09 (br s, 1H, H-5), 9.79 (s, 1H, H-1), 8.66 (br d, 1H, J = 6.8 Hz, H-3), 8.20 (dd, 1H, J = 2.2, 8.8 Hz, H-9), 8.03 (d, 1H, J = 7.0 Hz, H-6), 7.81 (dd, 1H, J = 4.2, 8.9 Hz, H-4), 7.58 (dt, 1H, J = 2.4, 9.1 Hz, H-7), 4.36 (s, 3H, methyl-H). ^{13}C NMR (126 MHz, DMSO-d_6) δ = 159.05, 157.15, 145.73, 139.81, 139.45, 137.84, 120.98, 120.89, 119.74, 119.70, 117.64, 117.44, 114.69, 114.62, 108.96, 107.74, 107.54, 46.76. HPLC/HRMS $[M]^+$ for $C_{12}H_{10}FN_2^+$ calculated 201.0823, found 201.0826.

2,8-Dimethyl-5H-pyrido[4,3-b]indole-2-ium iodide (**9c**). Yield 88%. t_R 8.16 min (Method A). ^{1}H NMR (DMSO-d_6, 250 MHz) δ = 12.95 (s, 1H, H-5), 9.76 (s, 1H, H-1), 8.6–8.7 (m, 1H, H-3), 8.1–8.2 (m, 1H, H-9), 8.00 (d, 1H, J = 7.0 Hz, H-6), 7.70 (d, 1H, J = 8.2 Hz, H-4), 7.5–7.6 (m, 1H, H-7), 4.37 (s, 3H, N—C$\underline{H_3}$), 2.5–2.6 (m, 3H, C—C$\underline{H_3}$). ^{13}C NMR (126 MHz, DMSO-d_6) δ = 144.93, 139.50, 138.95, 138.81, 131.86, 130.79, 121.34, 120.26, 119.79, 112.79, 108.47, 46.61, 21.10. HPLC/HRMS $[M]^+$ for $C_{13}H_{13}N_2^+$ calculated 197.1073, found 197.1075.

8-Methoxy-2-methyl-5H-pyrido[4,3-b]indole-2-ium iodide (**9d**). Yield 48%. t_R 7.65 min (Method A). ^{1}H NMR (DMSO-d_6, 300 MHz) δ = 12.88 (s, 1H, H-5), 9.77 (s, 1H, H-1), 8.59 (dd, 1H, J = 1.2, 7.0 Hz, H-3), 7.9–8.0 (m, 2H, H-4, H-9), 7.69 (d, 1H, J = 8.9 Hz, H-6), 7.32 (dd, 1H, J = 2.5, 8.9 Hz, H-7), 4.34 (s, 3H, O-C$\underline{H_3}$), 3.88 (s, 3H, N-C$\underline{H_3}$). ^{13}C NMR (126 MHz, DMSO-d_6) δ = 155.47, 144.88, 139.15, 138.65, 135.80, 120.92, 119.93, 118.72, 113.98, 108.54, 104.10, 55.73, 46.58. HPLC/HRMS $[M]^+$ for $C_{13}H_{13}IN_2O^+$ calculated 213.1022, found 213.1022.

2-Benzyl-5H-pyrido[4,3-b]indole-2-ium bromide (**9e**). To a solution of 50 mg compound **8a** (297 μmol, 1 equiv.) in acetone (34 mL) benzyl bromide (260 mg, 1.52 mmol, 5 equiv.) was added. The mixture was stirred for 12 h. The resulting colorless precipitate was filtered and washed with acetone yielding **9e** (10.1 mg, 40 μmol, 13%) as a colorless crystalline solid. t_R 6.63 min (Method B). ^{1}H NMR (CD_3OD, 250 MHz) δ = 9.8–9.9 (m, 1H, H-1), 8.70 (dd, 1H, J = 1.4, 7.0 Hz, H-3), 8.39 (d, 1H, J = 7.9 Hz, H-9), 7.96 (d, 1H, J = 7.0 Hz, H-6), 7.7–7.8 (m, 2H, H-4, H-7), 7.4–7.6 (m, 6H, H-8, benzyl-H), 5.87 (s, 2H, benzyl-H). ^{13}C NMR (126 MHz, CD_3OD) δ = 147.45, 143.37, 139.48, 139.10, 136.31, 131.28, 130.75, 130.73, 130.69, 130.66, 129.71, 129.67, 124.47, 123.16, 122.90, 121.94, 114.20, 114.16, 110.13, 64.46. HPLC/HRMS $[M]^+$ for $C_{18}H_{15}N_2^+$ calculated 259.1230, found 259.1233.

4.1.8. Synthesis of compound 10.

Synthesis of compound **10** has been described previously.[18]

4.2. Biological assays

4.2.1. Cell-based NMDA receptor assay

The cell-based assay of glutamate-induced excitotoxicity was performed using transgenic mouse fibroblast cells stably expressing either human GluN1-1a/2A or GluN1-1a/NR2B receptors as described previously.[16] Excitotoxicity was quantified by measuring lactate dehydrogenase (LDH) activity in cell medium. 100% excitotoxicity is defined as LDH activity measured after incubation of cells with 10 μM of agonists L-glutamate and glycine in the absence of antagonists. 0% excitotoxicity refers to LDH activity in medium in the presence of agonists and 100 μM ketamine. All data were determined in at least three independent experiments and are expressed as IC_{50} ± SD. It was verified for all substances that they do not directly inhibit LDH.

4.2.2. Production of recombinant human AChE

The coding sequence of the synaptic isoform of hAChE was obtained from GenBank (accession number M55040). A DNA fragment containing the entire hAChE sequence (614 amino acids) including the authentic amino-terminal signal peptide was synthesized at Genscript (Piscataway, USA) and cloned into pcDNA3.1 in-frame with a carboxy-terminal FLAG tag. The plasmid was transfected into HEK293 cells using the Lipofectamine 3000 reagent from Invitrogen (Carlsbad, USA) and stable cell lines were established by continuous selection in DMEM containing 10% fetal calf serum and 1.5 mg/ml G418. There was no background AChE production detectable in untransfected cells grown in serum-free medium. Therefore, the supernatants of stably transfected HEK-293 cells cultured in serum-free medium were used as source for rhAChE in all assays.

4.2.3. Preparation of AChE from human erythrocytes

Freshly withdrawn peripheral blood of healthy adult human donors was provided by the Institute of Transfusion Medicine at the University Hospital Jena, Germany. The experimental protocol was approved by the ethical committee of the University Hospital Jena. All methods were performed in accordance with the relevant guidelines and regulations. Erythrocyte membranes containing hAChE ("ghosts") were prepared essentially according to the protocol provided by Salazar et al.[29]. Briefly, blood was centrifuged at 2500*g* and the erythrocyte fraction was harvested. The erythrocytes were washed 4 times with 10 volumes of 0.9% NaCl. Next, erythrocytes were hemolyzed with 5 volumes hemolysis buffer (5 mM phosphate buffer, pH 7.4, 1 mM Na_2EDTA). Hemoglobin was removed by repeated centrifugation (15,000*g* for 16 min) and erythrocyte membrane concentrates (~4 mg/ml protein) were stored at −20 °C.

4.2.4. Cholinesterase measurements

Cholinesterase activities were measured using the Ellman assay as described previously,[16] by using supernatant of recombinant hAChE-expressing cells cultured in serum-free medium. Equine BChE was obtained from Sigma Aldrich (St. Louis, USA). All measurements were done in triplicates and are expressed as IC_{50} values ± SD.

4.3. Docking studies

The model of equine BChE (Uniprot Q9N1N9) was built using modeller[30] version 9.11 based on the available crystal structure of human BChE in complex with tacrine (PDB 4BDS). Sequence alignment was carried out in MOE v.2016.8 (Chemical Computing Group ULC, Montreal, Canada). The obtained alignment file was used to build the homology model of equine BChE where the cocrystallized ligand was kept during the homology modelling procedure. Equine and human BChE are 90% identical along the entire sequence. The substrate binding site contains only two mutations: Pro285 and Phe398 of human BChE are replaced by Leu313 and Ile426 in equine BChE, respectively.

The model of equine BChE described above and the crystal structure of AChE from *Torpedo californica* (TcAChE; PDB ID: 2CKM) were used in docking studies. The model was set up by using Schrödinger's Protein Preparation Wizard software package (Schrödinger Suite 2019–1, Schrödinger, New York, USA, NY, 2019) by adding hydrogen atoms, assigning protonation states, and minimizing the protein energy. All conserved water molecules in the active gorge were kept. Subsequently, the hydrogen bond networks and amino acid residue protonation states were optimized using PROPKA, and the complex was finally subjected to energy minimization using the OPLS3e force field in the default settings. Finally, receptor grids were generated using the default settings by assigning the cocrystallized ligand as the center of the grid. Ligands were first prepared using LigPrep (Schrödinger Release 2019–1: LigPrep, Schrödinger, LLC, New York, NY, 2019). Twenty conformers for each

ligand were subsequently generated using ConfGen. Molecular docking was performed using Glide (Schrödinger Release 2019–1: Glide, Schrödinger, LLC, New York, NY, 2019) in the Standard Precision mode to dock the generated ligand conformations into the prepared protein structures. Default settings without any constraints were used, the number of docking poses for post-docking minimization per ligand was increased to 20, and the maximal number of output poses per ligand was set to 2.

Funding

I.R. gratefully acknowledges a Ph.D. fellowship from the state of Thuringia ("Landesgraduiertenstipendium").

Institutional Review Board Statement: Not applicable.

CRediT authorship contribution statement

Sigrid Schwarthoff: Investigation, Data curation, Writing – original draft. **Nicolas Tischer:** Investigation. **Henrike Sager:** Investigation. **Bianca Schätz:** Investigation. **Marius M. Rohrbach:** Investigation. **Ihar Raztsou:** Investigation. **Dina Robaa:** Investigation, Visualization. **Friedemann Gaube:** Data curation, Supervision. **Hans-Dieter Arndt:** Resources, Supervision. **Thomas Winckler:** Conceptualization, Resources, Writing - review & editing.

Declaration of Competing Interest

The authors declare that they have no known competing financial interests or personal relationships that could have appeared to influence the work reported in this paper.

Acknowledgments

We are grateful to Heidemarie Graf and Anke Hinsching for expert technical assistance.

Appendix A. Supplementary material

Supplementary data to this article can be found online at https://doi.org/10.1016/j.bmc.2021.116355.

References

1 Alzheimer's Disease International. World Alzheimer Report 2019: Attitudes to dementia. Alzheimer's Disease International (ADI); 2019. https://www.alzint.org/u/WorldAlzheimerReport2019.pdf.
2 Arvanitakis Z, Shah RC, Bennett DA. Diagnosis and management of dementia: review. *JAMA*. 2019;322:1589–1599.
3 Cummings JL. Alzheimer's disease. *N Engl J Med*. 2004;351:56–67.
4 Lane CA, Hardy J, Schott JM. Alzheimer's disease. *Eur J Neurol*. 2018;25:59–70.
5 Greig NH, Utsuki T, Ingram DK, et al. Selective butyrylcholinesterase inhibition elevates brain acetylcholine, augments learning and lowers Alzheimer beta-amyloid peptide in rodent. *Proc Natl Acad Sci USA*. 2005;102:17213–17218.
6 Ballard CG, Greig NH, Guillozet-Bongaarts AL. Cholinesterases: roles in the brain during health and disease. *Curr Alzheimer Res*. 2005;2:281–290.
7 Lane RM, Potkin SG, Enz A. Targeting acetylcholinsterase and butyrylcholinesterase in dementia. *Int J Neuropsychopharmacol*. 2006;9:101–124.
8 Li Q, Yang H, Chen Y, Sun H. Recent progress in the identification of selective butyrylcholinesterase inhibitors for Alzheimer's disease. *Eur J Med Chem*. 2017;132:294–309.
9 Jasiecki J, Targońska M, Wasąg B. The role of butyrylcholinesterase and iron in the regulation of cholinergic network and cognitive dysfunction in Alzheimer's disease pathogenesis. *Int J Mol Sci*. 2021;22:2033.
10 Parsons CG, Danysz W, Dekundy A, Pulte I. Memantine and cholinesterase inhibitors: complementary mechanisms in the treatment of Alzheimer's disease. *Neurotox Res*. 2013;24:358–369.
11 Deardorff WJ, Grossberg GT. A fixed-dose combination of memantine extended-release and donepezil in the treatment of moderate-to-severe Alzheimer's disease. *Drug Des Devel Ther*. 2016;10:3267–3279.
12 Geerts H, Grossberg GT. Pharmacology of acetylcholinesterase inhibitors and N-methyl-D-aspartate receptors for combination therapy in the treatment of Alzheimer's disease. *J Clin Pharmacol*. 2006;46:8S–16S.
13 Matsunaga S, Kishi T, Nomura I, et al. The efficacy and safety of memantine for the treatment of Alzheimeŕs disease. *Expert Opin Drug Saf*. 2018;17:1053–1061.
14 Owen RT. Memantine and donepezil: a fixed drug combination for the treatment of moderate to severe Alzheimer's dementia. *Drugs Today (Barc)*. 2016;52:239–248.
15 Patel L, Grossberg GT. Combination therapy for Alzheimer's disease. *Drugs Aging*. 2012;28:539–546.
16 Otto R, Penzis R, Gaube F, et al. Evaluation of homobivalent carbolines as designed multiple ligands for the treatment of neurodegenerative disorders. *J Med Chem*. 2015;58:6710–6715.
17 Makhaeva GF, Lushchekina SV, Boltneva NP, et al. Conjugates of gamma-Carbolines and Phenothiazine as new selective inhibitors of butyrylcholinesterase and blockers of NMDARs for Alzheimer Disease. *Sci Rep*. 2015;5:13164.
18 Otto R, Penzis R, Gaube F, et al. Beta and gamma carboline derivatives as potential anti-Alzheimer agents: a comparison. *Eur J Med Chem*. 2014;87:63–70.
19 Greenblatt HM, Dvir H, Silman I, Sussman JL. Acetylcholinesterase: a multifaceted target for structure-based drug design of anticholinesterase agents for the treatment of Alzheimer's disease. *J Mol Neurosci*. 2003;20:369–383.
20 Cheung J, Rudolph MJ, Burshteyn F, et al. Structures of human acetylcholinesterase in complex with pharmacologically important ligands. *J Med Chem*. 2012;55:10282–10286.
21 Rosenberry TL, Brazzolotto X, Macdonald IR, et al. Comparison of the binding of reversible inhibitors to human butyrylcholinesterase and acetylcholinesterase: a crystallographic, kinetic and calorimetric study. *Molecules*. 2017;22:2098.
22 Nicolet Y, Lockridge O, Masson P, Fontecilla-Camps JC, Nachon F. Crystal structure of human butyrylcholinesterase and of its complexes with substrate and products. *J Biol Chem*. 2003;278:41141–41147.
23 Colletier JP, Sanson B, Nachon F, et al. Conformational flexibility in the peripheral site of Torpedo californica acetylcholinesterase revealed by the complex structure with a bifunctional inhibitor. *J Am Chem Soc*. 2006;128:4526–4527.
24 Greenblatt HM, Guillou C, Guénard D, et al. The complex of a bivalent derivative of galanthamine with torpedo acetylcholinesterase displays drastic deformation of the active-site gorge: implications for structure-based drug design. *J Am Chem Soc*. 2004;15405–15411.
25 Zha X, Lamba D, Zhang L, et al. Novel tacrine-benzofuran hybrids as potent multitarget-directed ligands for the treatment of Alzheimer's disease: design, synthesis, biological evaluation, and X-ray crystallography. *J Med Chem*. 2016;59:114–131.
26 Rydberg EH, Brumshtein B, Greenblatt HM, et al. Complexes of alkylene-linked tacrine dimers with Torpedo californica acetylcholinesterase: binding of Bis5-tacrine produces a dramatic rearrangement in the active-site gorge. *J Med Chem*. 2006;49:5491–5500.
27 Kalin JH, Butler KV, Akimova T, Hancock WW, Kozikowski AP. Second-generation histone deacetylase 6 inhibitors enhance the immunosuppressive effects of Foxp3+ T-regulatory cells. *J Med Chem*. 2012;55:639–651.
28 Sardessai MS, Brander MJ, Midha KK, Hawes EM. Synthesis of deuterium labelled fluphenazine utilising borane reduction. *J Lab Comp Radiopharm*. 1986;23:317–327.
29 Salazar PB, de Athayde Moncorvo Collado A, Canal-Martínez V, Minahk CJ. Differential inhibition of human erythrocyte acetylcholinesterase by polyphenols epigallocatechin-3-gallate and resveratrol. Relevance of the membrane-bound form. *Biofactors*. 2017;43:73–81.
30 Sali A, Blundell TL. Comparative protein modelling by satisfaction of spatial restraints. *J Mol Biol*. 1993;234:779–815.